An IIR-Filter Approach to Time Variant PLC-Channel Modelling

Gabriel Moreno-Rodríguez*, Lars T. Berger*,
* Design of Systems on Silicon (DS2),
C/. Charles Robert Darwin 2, Parc Tecnològic,
46980 Paterna, Valencia, SPAIN.
gabriel . moreno @ ds2 . es, lars . berger @ ds2 . es

Abstract— A physically based power line communication channel model is derived. Elements within a power line network, *e.g.* line discontinuities, branches, and loads, are modelled as IIR-filters. The transfer function of the overall channel is calculated by concatenating the transfer functions of the individual elements. In a second step time variation is modelled through load impedances changes. It is shown that wide band load impedance measurements over the period of several AC mains-cycles can be easily integrated to deliver a deterministic cyclostationary power line channel model.

Keywords— Cyclostationarity, impedance change, infinite impulse response, power line channel modelling, load impedance, transmission line.

I. INTRODUCTION

Since the late 90s an increased effort has been put onto the characterization of *power line communication* (PLC) channels with the aim of designing communication systems that use the electric power distribution grid as data transmission medium.

In terms of power line channel modelling one can distinguish between *parametric* and *physical* models. Parametric models use a high level of abstraction, and describe the channel, for example, through its impulse response characteristics [1]–[3]. Hence, parametric models usually provide a high level of understanding and are especially well suited for stochastic simulations. On the other hand, physical models describe the electric properties of a transmission line, *e.g.* through the specification of cable parameters, cable length and the position of branches, *etc.* [4]–[7]. Physical models are therefore especially well suited to represent and test deterministic power line situations and will be at the center of attention throughout this publication.

Most physical models are based on representing power line elements and connected loads in form of their *ABCD* or *S-parameters*, which are subsequently interconnected to produce the channel's frequency response [4]–[7]. Alternatively, Section II describes power line elements as well as connected loads as *infinite impulse response* (IIR) filters, which is a novel and still intuitive approach if one considers that a communication signal travels in form of an electromagnetic wave over the PLC channel and may bounce an infinite amount of times between neighboring line discontinuities. Section III outlines how to concatenate the introduced individual IIR-filter elements to form complex power line networks. To validate

the novel approach a deterministic power line network is simulated in Section IV and its frequency and impulse response are compared against PSpice simulations. To introduce time variation, which is often due to load impedance changes [8], Section V presents example measurement results of a time variant halogen lamp impedance and outlines how impedance measurements in general can be integrated into the IIR-filter approach. Finally, Section VI presents examples of dynamic power line channel simulation results.

II. IIR-FILTER REPRESENTATION

Consider the open stub line example in Fig. 1 adapted from [1]. An impedance matched transmitter is placed at A. An impedance matched receiver is placed at C. Hence, in this simple example there is no need to bother about impedance discontinuities at the input and the output of the network. D represents a 70 Ω parallel load. B marks the point of an electrical T-junction. l_x and Z_x, with $x \in [1, 2, 3]$, represent the line lengths and characteristic impedances. t_{xy} and r_{xy}, with $y \in [B, D]$, indicate the transmission and reflection coefficients encountered at impedance discontinuities respectively, whose dependencies on the characteristic impedances are derived in [9]. Generally, at an impedance discontinuity from Z_a to Z_b the transmission and reflection coefficients are given by

$$r_{ab} = \frac{Z_b - Z_a}{Z_b + Z_a} \quad , \tag{1}$$
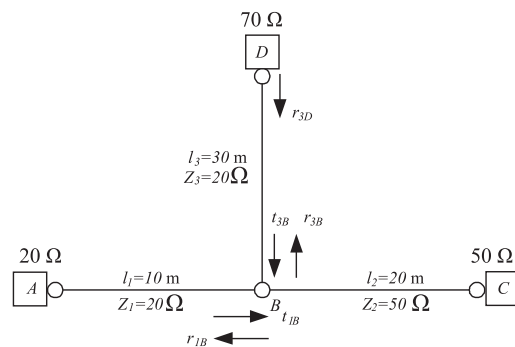
$$t_{ab} = 1 + r_{ab} \quad . \tag{2}$$

Fig. 1. Simple stub line example.

Specifically for the situation in Fig. 1 r_{1B} is given by

$$r_{1B} = \frac{(Z_2 \parallel Z_3) - Z_1}{(Z_2 \parallel Z_3) + Z_1} \quad , \quad (3)$$

where $(Z_2 \parallel Z_3)$ represents the joint impedance of Z_2 and Z_3 when connected in parallel.

A power-line communication signal travels in form of a direct wave from A over B to C. Another wave travels from A over B to D, bounces back to B and reaches C. All further waves travel from A to B, and undergo multiple bounces between B and D before they finally reach C. The number of bounces between B and D is infinite, motivating the idea that an infinite impulse response filter (IIR) can be used to represent the power line network. Considering the reflection and transmission coefficients as gains, and considering ideal transmission lines, whose lengths relate to pure time delays, the simple stub line example may be transformed into an IIR-filter as displayed in Fig. 2. In Fig. 2 boxes represent delays and triangles represent filter coefficients.

A time discrete representation is considered. The smallest time step T_s relates to the system's sampling frequency via $f_s = \frac{1}{T_s}$. Thus, every line length relates to a delay which, measured in samples, can be expressed as

$$N_{delay,x} = \frac{delay_x}{T_s}$$
$$= \frac{l_x}{T_s \cdot v_x} \quad , \quad (4)$$

where l_x and v_x represent the length and the wave speed of line x respectively. The filter from Fig. 2 may be expressed through its z-transfer function where a time delay is given as $z^{-\mathrm{Round}\left\{\frac{l_x}{T_s \cdot v_x}\right\}}$. $\mathrm{Round}\{\ \cdot\ \}$ stands for rounding to the nearest integer. Instead of using this lengthy notation the z-transform of the time delay caused by line length l_x is denoted z^{-l_x} for brevity. The z-transfer functions of the subfilter blocks marked in Fig. 2 as H_a to H_d are

$$H_a = t_{1B} \cdot z^{-l_1} \quad , \quad (5)$$

$$H_b = 1 \quad , \quad (6)$$

$$H_c = \frac{t_{3B} \cdot r_{3D} \cdot z^{-2 \cdot l_3}}{1 - r_{3B} \cdot r_{3D} \cdot z^{-2 \cdot l_3}} \quad , \quad (7)$$
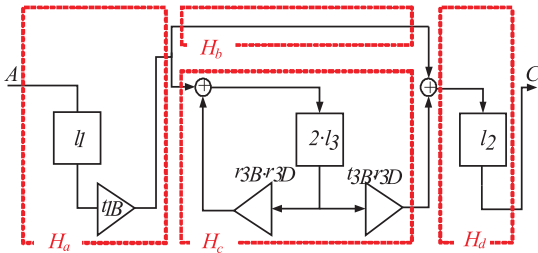
$$H_d = z^{-l_2} \quad . \quad (8)$$

Considering that the sub-filter blocks H_b and H_c lie in parallel and are concatenated in serial with H_a and H_d the overall z-transfer function of the simple stub line example writes

$$H = H_a \cdot (H_b + H_c) \cdot H_d$$

$$= t_{1B} \cdot z^{-l_1} \cdot z^{-l_2} \cdot \left(1 + \frac{t_{3B} \cdot r_{3D} \cdot z^{-2l_3}}{1 - r_{3B} \cdot r_{3D} \cdot z^{-2l_3}} \right)$$

$$= \frac{\begin{pmatrix} t_{1B} \cdot z^{-(l_1+l_2)} \\ + (t_{3B} \cdot r_{3D} - r_{3B} \cdot r_{3D}) \\ \cdot t_{1B} \cdot z^{-(l_1+l_2+2l_3)} \end{pmatrix}}{1 - r_{3B} \cdot r_{3D} \cdot z^{-2l_3}}$$

$$. \quad (9)$$

The so derived H is the feed-forward filter of the stub line from input A to output B. In the following all feed-forward filters from input to output are denoted H_f.

III. MODELLING COMPLEX POWER LINE NETWORKS

Usually power line networks consist of much more complex structures than that presented in the stub line example. Often electrical grids show multiple parallel impedance terminations, wire divisions into multiple lines, as well as serial impedances. Nevertheless, it is still possible to fully describe each of these primary elements as an IIR-filter with its own primary transfer function. The overall complex transfer function is then obtained through concatenation of the primary transfer functions.

As one may not generally assume that input and output impedances of the primary element are matched it is not sufficient to describe each primary element by its feed-forward filter only. Additionally, as sketched in Fig. 3, a filter that describes wave propagation into the input port and then the reflection back out of it is needed and will be denoted $\tilde{H}_b$. Further, a filter that describes wave propagation into the output port and the reflection back out of it is denoted $\tilde{H}_f$. And finally the backward filter describing wave propagation into the output port and out of the input port is denoted H_b.

Using the same inspection technique as in the stub line example, *i.e.* IIR-filter representation based on coefficients and time delays, all feed-forward and feedback filters are obtained for primary power line elements such as a *lossless line*, an

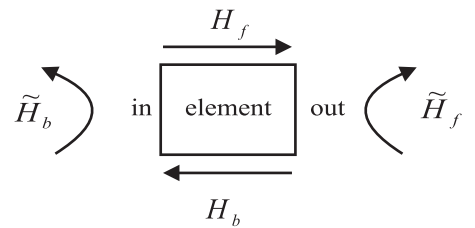Fig. 2.   IIR-filter representation of stub line example.
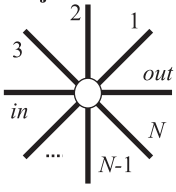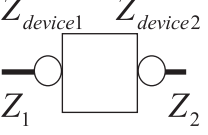

Fig. 3.   Feed-forward and feedback filter definitions.
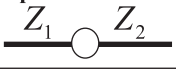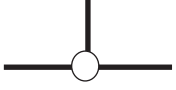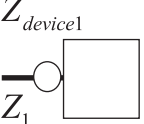
Primary element	Comment	H_f	H_b	$\widetilde{H}_f$	$\widetilde{H}_b$
Lossless line l	line length l	z^{-l}	z^{-l}	0	0
Impedance discontinuety $Z_1 \quad Z_2$	line lengths zero	$\dfrac{2 \cdot Z_2}{Z_2 + Z_1}$	$\dfrac{2 \cdot Z_1}{Z_1 + Z_2}$	$\dfrac{Z_1 - Z_2}{Z_1 + Z_2}$	$\dfrac{Z_2 - Z_1}{Z_2 + Z_1}$
T-junction	line lengths zero, with the same labels as in Fig.1, $\widetilde{H}_{bD}$ is the filter at port D back into junction	$\dfrac{t_{2B} + \left(t_{3B} - r_{3B}\right)t_{2B}\widetilde{H}_{bD}}{1 - \widetilde{H}_{bD}r_{3B}}$ $\dfrac{t_{1B} + \left(t_{3B} - r_{3B}\right)t_{1B}\widetilde{H}_{bD}}{1 - \widetilde{H}_{bD}\cdot r_{3B}}$	$\dfrac{r_{2B} + \left(t_{2B}t_{3B} - r_{2B}r_{3B}\right)\widetilde{H}_{bD}}{1 - r_{3B}\widetilde{H}_{bD}}$ $\dfrac{r_{1B} + \left(t_{1B}t_{3B} - r_{1B}r_{3B}\right)\widetilde{H}_{bD}}{1 - r_{3B}\widetilde{H}_{bD}}$		
Star-junction	See Sec. III for explanation of elements	$t_{out}\cdot(1 + \sum_{i=1}^{N}\widetilde{H}''_{bi})$ $t_{in}\cdot(1 + \sum_{i=1}^{N}\widetilde{H}''_{bi})$	$r_{out} + t_{out}\cdot(\sum_{i=1}^{N}\widetilde{H}''_{bi})$ $r_{in} + t_{in}\cdot(\sum_{i=1}^{N}\widetilde{H}''_{bi})$		
Serial impedance $Z_{device1} \quad Z_{device2}$ $Z_1 \qquad Z_2$	$Z_{device1}, Z_{device2}$ input impedances seen from left/right. Z_1, Z_2 line impedances	$\dfrac{2 \cdot Z_{device1}}{Z_{device1} + Z_1}$	$\dfrac{2 \cdot Z_{device2}}{Z_{device2} + Z_2}$	$\dfrac{Z_{device2} - Z_2}{Z_{device2} + Z_2}$	$\dfrac{Z_{device1} - Z_1}{Z_{device1} + Z_1}$
Parallel impedance $Z_{device1}$ Z_1	$Z_{device1}$ input impedances of load. Z_1 line impedances	$\dfrac{2 \cdot Z_{device1}}{Z_{device1} + Z_1}$	0	0	$\dfrac{Z_{device1} - Z_1}{Z_{device1} + Z_1}$

Fig. 4. Summary of the transfer functions of primary power line elements.

impedance discontinuity, a *T-junction*, a more general *star-junction* as well as a *serial* and a *parallel impedance*. The corresponding transfer functions are summarised in Fig. 4.

To obtain a modular structure line discontinuities, as well as T-, and star-junctions are described assuming fictitious zero length lines. In a second step any line length combination can be achieved through concatenation with lossless line primary elements.

The star-junction from Fig. 4 is the most complicated of the presented primary elements and deserves some further explanation. It can be defined as a connection of $N+2$ lines in a center point, denoted Cen. One port of the star is designated as input in, another as output out. Every line has its own characteristic impedance Z_x with $x \in [1, \ldots N]$ and Z_{in}, Z_{out}. A wave advancing in the direction of port x experiences the corresponding $\widetilde{H}_{bx}$. The feed-forward and feedback filters from port in to out are based on the following definitions:

t_x, t_{in}, t_{out} as well as r_x, r_{in}, r_{out} are the transmission and reflection coefficients for a wave travelling from line x, in, or

out into the junction. The impedance mismatch experienced by the wave is between its current line impedance and the parallel impedance of the remaining $N + 1$ lines. Further,

$$\widetilde{H}''_{bx} = \widetilde{H}'_{bx} \cdot \frac{\prod\limits_{\substack{i=1 \\ i \neq x}}^{N}\left(1 + \widetilde{H}'_{bi}\right)}{\prod\limits_{\substack{i=1 \\ i \neq x}}^{N}\left(1 + \widetilde{H}'_{bi}\right) - \left(1 + \widetilde{H}'_{bx}\right)\sum\limits_{\substack{i=1 \\ i \neq x}}^{N}\left(\frac{\widetilde{H}'_{bi}}{(1+\widetilde{H}'_{bi})}\left(\prod\limits_{\substack{k=1 \\ k \neq i}}^{N}\left(1 + \widetilde{H}'_{bk}\right)\right)\right)},$$

(10)

where $\widetilde{H}'_{bx}$ is given by

$$\widetilde{H}'_{bx} = \frac{t_x \cdot \widetilde{H}_{bx}}{1 - r_x \cdot \widetilde{H}_{bx}} \quad . \tag{11}$$

After defining all the primary elements, a complex network can be constructed by concatenation of their z-transfer functions. Concatenation of any two elements follows the rules for filter concatenation in their cascade and parallel form

[10]. Specifically, indexing all transfer functions of any two elements with the subscripts $_1$ and $_2$, and the resulting transfer functions with the subscript $_{1,2}$, the following concatenation rules apply:

$$H_{f1,2} = \frac{H_{f1} \cdot H_{f2}}{1 - \tilde{H}_{f1} \cdot \tilde{H}_{b2}} \quad , \quad (12)$$

$$H_{b1,2} = \frac{H_{b2} \cdot H_{b1}}{1 - \tilde{H}_{b2} \cdot \tilde{H}_{f1}} \quad , \quad (13)$$

$$\tilde{H}_{f1,2} = \tilde{H}_{f2} + \frac{H_{b2} \cdot \tilde{H}_{f1} \cdot H_{f2}}{1 - \tilde{H}_{b2} \cdot \tilde{H}_{f1}} \quad , \quad (14)$$

$$\tilde{H}_{b1,2} = \tilde{H}_{b1} + \frac{H_{f1} \cdot \tilde{H}_{b2} \cdot H_{b1}}{1 - \tilde{H}_{f1} \cdot \tilde{H}_{b2}} \quad . \quad (15)$$

Concatenation of more than two elements is achieved by iterative application of (12) to (15).

IV. STATIC IIR-FILTER MODEL VALIDATION

Using the expressions from Section III the simple stub line example from Fig. 1 as well as a more complex power line network displayed in Fig. 5 have been simulated. Additionally, to validate the IIR-filter based modelling strategy PSpice implementations of the networks have been obtained using common resistors, voltage source and transmission line components provided in the PSpice libraries. The PSpice frequency transfer function was obtained with an *AC-Sweep*, while the impulse response was obtained by exciting with a voltage impulse that approximates a delta function. As this impulse did not resemble an ideal delta with unit energy the obtained PSpice impulse response was afterwards power normalised. The corresponding results are compared in Fig. 6. It can be seen that a good match is obtained in all cases which underlines the validity of the novel IIR-filter based approach.

V. DYNAMIC IIR-FILTER MODELS BASED ON LOAD REFLECTION COEFFICIENT MEASUREMENTS

Till now the aspect of time dynamics has been neglected. However, loads, such as a halogen lamp connected to the electrical grid, change their input impedance synchronously as a function of the AC-mains cycle, causing cyclostationary channel variations [8], [11]. To capture such dynamics the IIR-filter based model cyclically switches between different linear time invariant IIR-filter representations. This is usually considered a valid approximation as long as the impulse response length is by several orders of magnitude smaller than the channel's coherence time [12]. The channel coherence
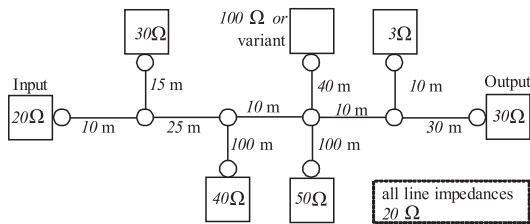
time lies in the order of ms [13]. However, when modelling the channel with IIR-filters the impulse response is infinite. Nevertheless, as seen in Fig. 6, and as confirmed for typical power line networks in [1], [2], the impulse response power tends to zero within μs so that the same *slow variation hypothesis* as used in [12] applies.

The following presents in form of an example how wideband time variant load reflection coefficient measurements may be integrated into the overall modelling framework. More specifically, wideband measurements of the reflection coefficient of a halogen lamp are obtained using a network analyser. Fig. 8 displays the measured reflection coefficient at three example timings, *i.e.* at 3.5 msec, 7 msec and 14 ms. The measured coefficients are approximated with IIR-filters using standard digital filter design software tools. The so obtained approximated reflection coefficients are also plotted in Fig. 8.

Denote the measured reflection coefficient as $\Gamma_{measured}$ and its approximated z-transfer function as Γ_{approx}. Further, denote the network analyser characteristic reference impedance as Z_0. The input impedance of the device may then be approximated as

$$Z_{in} = Z_0 \cdot \frac{1 - \Gamma_{approx}}{1 + \Gamma_{approx}} \quad . \quad (16)$$

This impedance can be substituted in the parallel impedance equations from Fig. 4 to obtain $\tilde{H}_b$, which is the z-transfer function of the filter.

Once the primary element z-transfer functions description of the parallel impedances has been obtained with the desired time step granularity it can be readily integrated into the overall filter description using the concatenation rules from Section III.

VI. TIME VARIANT SIMULATION RESULTS

The power line network from Fig. 1 has been simulated connecting the halogen lamp at point D. Three realisations of the corresponding frequency transfer function are displayed in Fig. 7 (a).

Similarly, the halogen lamp has been connected in the complex power line network from Fig. 5 at the point labelled '100Ω or variant'. The corresponding frequency transfer function is presented in Fig. 7 (b).

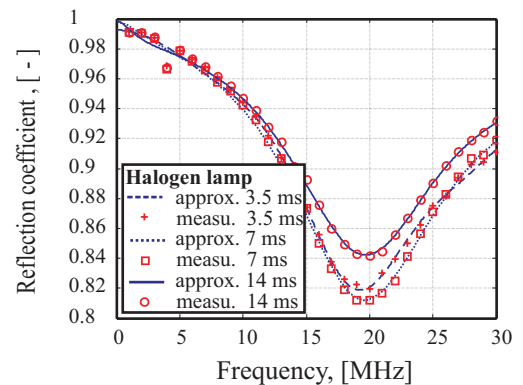Fig. 5. Complex power line network example.

Fig. 8. Wideband halogen lamp reflection coefficient measurements.
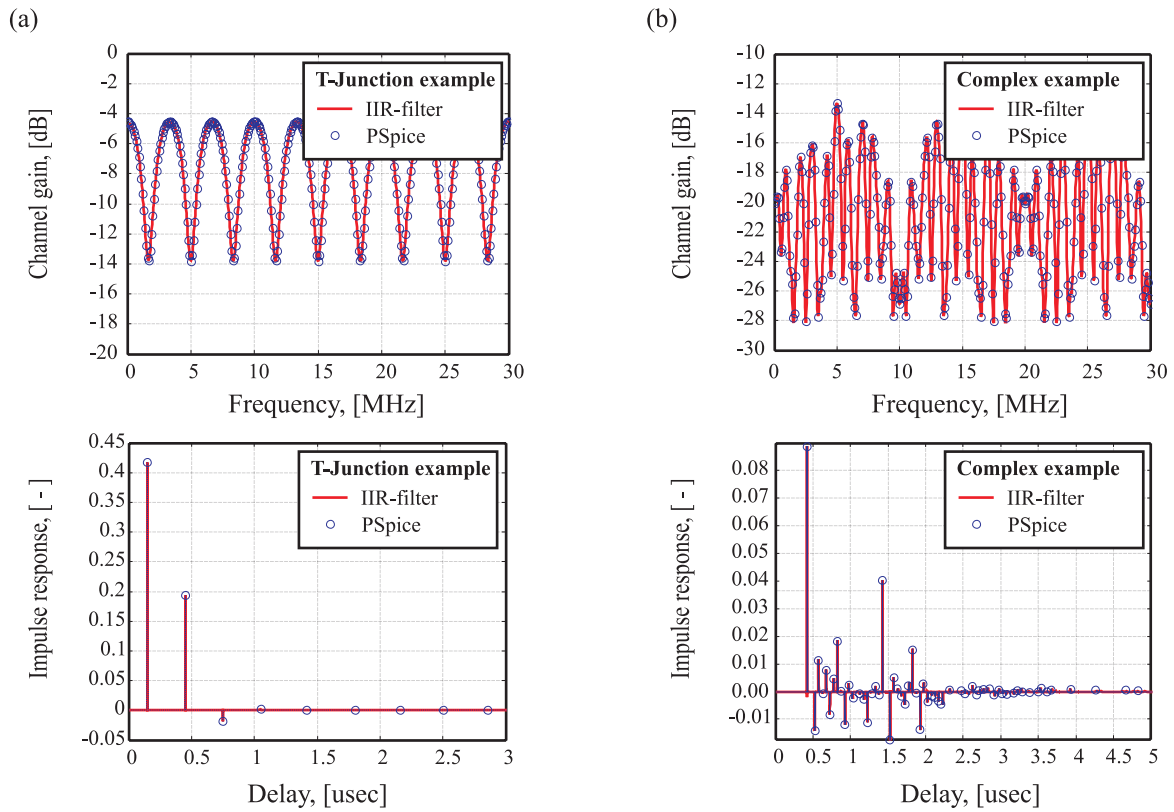
Fig. 6.   IIR-based and PSpice based frequency and impulse response of (a) the stub line example, (b) the complex network example.
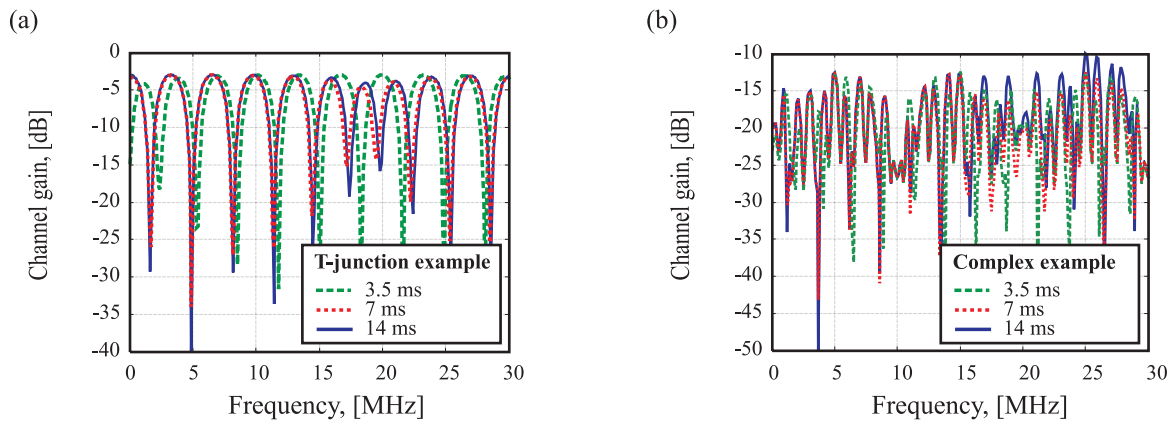

Fig. 7.   Time variation of the frequency response for (a) the stub line example and (b) the complex network example.

Both figures indicate that only a single halogen lamp can already cause significant temporal variation of the power line channel.

VII. Conclusions

A physically based IIR-filter representation of power line channels has been introduced as an alternative to more traditional ABCD or S-parameter formulations. Using this IIR-filter approach measured wide band time variant loads can easily be integrated into the channel modelling process. The proposed IIR-filter representation has been validated against PSpice simulations. It was shown that physically based deterministic models of the power line channel can be obtained that are able to model cyclostationary power line channel variations. The addition of random processes for network generation and load placement would further permit a stochastic channel model extension.

VIII. Acknowledgements

REFERENCES

[1] M. Zimmermann and K. Dostert, "A Multi-Path Signal Propagation Model for the Power Line Channel in the High Frequency Range", in *International Symposium on Power-line Communications and its Applications*, Lancaster, UK, April 1999, pp. 45–51.

[2] H. Philipps, "Development of a Statistical Model for Powerline Communication Channels", in *International Symposium on Power Line Communications (ISPLC)*, Limerick, Ireland, April 2000, pp. 153–160.

[3] M. Babic, M. Hagenau, K. Dostert, and J. Bausch, "Theoretical postulation of PLC channel model", IST Integrated Project Deliverable D4v2.0, The OPERA Consortium, March 2005.

[4] T. Esmailian, F. R. Kschischang, and P. G. Gulak, "An In-building Power Line Channel Simulator", in *International Symposium on Power Line Communications and Its Applications (ISPLC)*, Athens, Greece, March 2002.

[5] S. Galli and T. Banwell, "A novel approach to the modeling of the indoor power line channel-Part II: transfer function and its properties", *IEEE Transactions on Power Delivery*, vol. 20, no. 3, pp. 1869 – 1878, July 2005.

[6] T. Sartenaer and P. Delogne, "Deterministic modeling of the (shielded) outdoor power line channel based on the multiconductor transmission line equations", *IEEE Journal on Selected Areas in Communications*, vol. 24, no. 7, pp. 1277–1291, July 2006.

[7] S. Barmada, A. Musolino, and M. Raugi, "Innovative model for time-varying power line communication channel response evaluation", *IEEE Journal on Selected Areas in Communications*, vol. 7, no. 24, pp. 1317–1326, July 2006.

[8] F. J. Canete Corripio, J. A. Cortes Arrabal, L. Diez del Rio, and J. T. Entrambasaguas Munoz, "Analysis of the cyclic short-term variation of indoor power line channels", *IEEE Journal on Selected Areas in Communications*, vol. 24, no. 7, pp. 1327 – 1338, July 2006.

[9] D. M. Pozar, *Microwave Engineering*, John Wiley & Sons, Inc., 3rd edition, 2005.

[10] A. V. Oppenheim, R. W. Schafer, and J. R. Buck, *Discrete-Time Signal Processing*, Signal Processing Series. Prentice Hall, 2nd edition, 1999.

[11] J. A. Cortes, F. J. Canete, L. Diez, and J. T. Entrambasaguas, "Characterization of the cyclic short-time variation of indoor power-line channels response", in *International Symposium on Power Line Communications and Its Applications (ISPLC)*, Vancouver, Canada, April 2005, pp. 326–330.

[12] S. Sancha, F. J. Canete, L. Diez, and J. T. Entrambasaguas, "A Channel Simulator for Indoor Power-line Communications", in *IEEE International Symposium on Power Line Communications and Its Applications*, Pisa, Italy, March 2007, pp. 104–109.

[13] S. Katar, B. Mashburn, K. Afkhamie, H. Latchman, and R. Newman, "Channel Adaptation based on Cyclo-Stationary Noise Characteristics in PLC Systems", in *IEEE International Symposium on Power Line Communications and Its Applications*, March 2006, pp. 16–21.